Research Journal of Material Sciences _____ ISSN 2320–6055
Vol. **3(2),** 1-8, June **(2015)** *Res. J. Material Sci.*

Kinetics Study on the Thermal Decomposition of Lanthanum Oxalate Catalysed by Zn-Cu Nano Ferrites

Nayak Himansulal
P.G. Department of Chemistry, Orissa University of Agriculture and Technology, Bhubaneswar 751003(Orissa), INDIA

Available online at: www.isca.in
Received 20th Apirl 2015, revised 20th May 2015, accepted 13th June2015

Abstract

*Nanostructured zinc-copper mixed ferrite was synthesized using sol-gel method. XRD patterns of different compositions of zinc copper ferrite, $Zn_{(1-x)}Cu_xFe_2O_4$ (x = 0.0, 0.25, 0.50, 0.75), revealed single phase inverse spinel ferrite in all the samples. With increasing copper concentration, the crystallite size increases from 30 nm to 50 nm. The surface morphology of all the samples studied by the Scanning Electron Microscopy showing porous structure of particles throughout the sample. The prepared samples were also analysed by XRD, FTIR, TEM. Catalytic activity of the prepared samples were studied on lanthanum oxalate decomposition by Thermogravimetric methods (TGA). The rate constant **'k'** has got the highest value with x=0.75 and 5 mol% concentration and highest value is attributed to high copper concentration and also due to ion pairs as a result of mutual charge interaction i.e. besides the one component sites Cu^{2+} –Cu^{+}, Fe^{3+} –Fe^{2+} , there will be also the mixed sites Cu^{2+} –Fe^{+} as well as Cu^{+} –Fe^{2+}. In other words, the increasing activity of mixed oxides is attributed to enhanced concentration of active sites by creating new ion pairs. With increasing Zn content increases particle size thereby providing comparatively less surface area for the catalytic activities due to large ionic radii of Zinc. Catalytic activity of ferrite powders changes remarkably due to the changes of the valence state of the components of the ferrites, responsible for catalytic activities and that oxidises the carbon monoxide released from Lanthanum oxalate*

Keywords: Mixed ferrite, Spinel, Valence induction, Catalyst activity, Rate constant, Lanthanum oxalate, Thermogravimetric study.

Introduction

Ferrites have wide range of applications in integrated circuitry, transformer cores, magnetic recording etc[1,2] The study of ferrites because of their novel properties and technological applications are immensely important when the size of the particles approaches to nanometer scale, due to the fundamental differences in their magnetic and electronic properties compared to the bulk counterparts. Nano oxides due to their electrical properties have been found to be good catalysts, as compared to their corresponding normal oxides. [3]

$Ni_{0.5}M_{0.5}Fe_2O_4$ (M = Co, Cu) ferrite nanoparticles synthesized using citrate precursor method annealed at temperatures 400°C, 450°C, 500°C and 550°C, display cubic spinel structure upto 450°C and at temperature higher than 450°C display a tetragonal structure suggesting that nucleation/growth mechanism is different at temperatures above and below a critical temperature in this range[4]. Further $Ni_{0.5}M_{0.5}Fe_2O_4$ ferrite doped with 0.1 and 0.4 mol of Cu behaves as a catalyst [5] and comparative analysis of the two catalysts indicated that the catalyst doped with 0.4 mol of Cu showed the better performance. The nickel substituted copper ferrite nanoparticles ($Ni_xCu_{1-x}Fe_2O_4$), where x = 0.0, 0.2, 0.4, 0.6, 0.8, 1.0) were found to have better catalytic activity as compared to the corresponding metal oxides[6]. A study on the thermal decomposition of the mixtures of lanthanum oxalate hydrate and transition metal nano oxide compounds (TMNOCs) viz. CuO, Fe_2O_3, TiO_2 and Cr_2O_3 of 5 mole% ratio has been carried out and the results reveal that other than CuO, the oxides have a retarding effect on the decomposition rate[7].

The Zn^{2+} substitution in ferrites i.e Cobalt–zinc ferrite nano-particles $Co_{1-x}Zn_xFe_2O_4$ observed variation in crystalline size and on the structural properties of ferrite nanoparticles[8]. The $Ni_{1-x}Cu_xFe_2O_4$ ferrites prepared by sol-gel method and sintered at high temperature show the effect of copper doping on the structural and magnetic properties of nickel ferrites, due to formation of single phase spinel ferrite structure[9]. Ferrospinels of nickel, cobalt and copper and their sulphated analogues prepared by co-precipitation route proved to be good catalysts for the benzoylation of toluene[10].

Properties of Crystalline Copper Zinc nano ferrites having cubic spinel structure are affected by several factors such as the chemical composition, electronic configuration, ionic radius, synthesis techniques etc. Copper ferrite ($CuFe_2O_4$) has been widely used as a potential catalysts for various applications,. Magnetic and electrical properties of Copper ferrites changes appreciably with chemical component and cation distribution e.g. bulk $CuFe_2O_4$ has an inverse spinel structure where B sites are occupied by 85% of Cu^{2+} cations, where as $ZnFe_2O_4$ being normal spinel Zn^{2+} ions preferentially occupy A sites and simultaneously Fe^{3+} ions are displaced from A sites for B sites.

Zn-substitution results in change of chemical composition and a different distribution of cations between A and B sites. Hence the magnetic and electrical properties of spinel ferrites changes with replacing cations[11].

Spinel ferrites are found to have semiconducting properties of n or p–type[12]. With a view to understand the conduction mechanism in mixed Cu-Zn ferrites, the semiconducting properties as a function of composition and temperature, the results for such a study towards lanthanum oxalate decomposition are presented in this paper. The aim of this work is to present an economical method of preparation of Cu-Zn ferrite by the citrate precursor method and to achieve sintering at lower temperatures. The present work also highlight on preparation of zinc ferrite nanopowders and replacing zinc sites by copper by self combustion method following by thermal treatment and to study the catalytic activity on lanthanum oxalate decomposition to CO and CO_2. The changes in the phase composition of materials after the catalytic test were also the focus of investigation. The relationship between parameter of synthesis, phase composition, particle size, microstrain and catalytic behavior of ferrite materials has been discussed.

Material and Methods

Preparation of lanthanum oxalate: Oxalates of La(III) was prepared as per our early work[13] using High purity AR grade $La(NO_3)_3$ and ammonium oxalate solution and finally dried at 100°C to a constant weight. Four samples with chemical compositions as $ZnFe_2O_4$, $Zn_{0.75}Cu_{0.25}Fe_2O_4$, $Zn_{0.50}Cu_{0.50}Fe_2O_4$, and $Zn_{0.25}Cu_{0.75}Fe_2O_4$ were prepared using $Zn(NO_3)_2{\cdot}6H_2O$, $Cu(NO_3)_2{\cdot}3H_2O$ and $Fe(NO_3)_3{\cdot}9H_2O$ as starting materials all being analytically pure.. Citric acid (AR Grade) used as chelating agent. The gel was calcined at 700°C for 6 hours in a furnace to obtain the flake type materials. The flakes were thoroughly grinded in agate mortar to get the powdered form of material . The prepared samples have been referred to as S1, S2, S3, and S4, respectively

Preparation of mixture: Mixtures of lanthanum oxalate was prepared with S1, S2, S3, and S4, in three different mole percentage i.e. 2, 5, and 10 Mol% by grinding and mixing them in an agate mortar. The mixtures of uniform mesh size were subjected to Thermogravimetric study using SCHIMADZU DTG 50 thermal analyser using linear rising temperature technique with 5°C min^{-1} as rate of heating.

Results and Discussions

X-Ray Diffraction Analysis*:* The observed XRD patterns of nano catalyst samples (figure-1) are in good agreement with the JCPDS card 82-1042 (table-1). The XRD pattern shows single peak corresponding to each diffraction angle; hence, it shows the single phase of inverse spinel zinc copper ferrite. XRD patterns indicate the crystallite size of the mixed ferrites increases on increasing the Copper concentration.

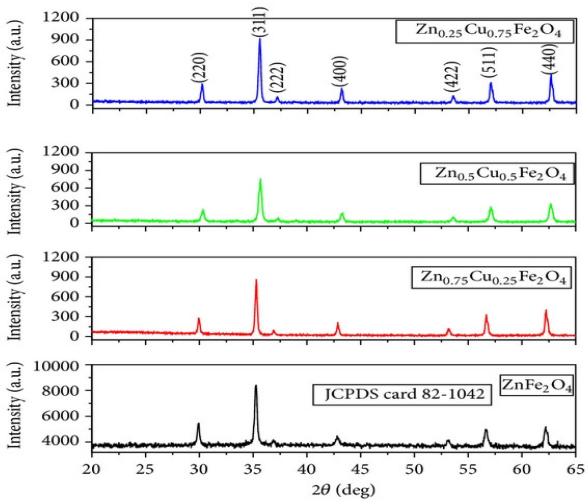

Figure-1
X- ray diffraction diagrams for various types of prepared Zn- Cu Ferrites

Table-1
XRD patterns of prepared Zn-Cu Ferrite The average particle diameter was found to be 30 nm which agrees well with that estimated from XRD data

Zn-Cu Ferrite	Position 2θ,deg	d spacing observed, Å	d spacing JCPDS,Å
$ZnFe_2O_4$	29.913	2.986	2.9851
	33.158	2.5517	2.5457
	36.877	2.4366	2.4347
	42.841	2.1102	2.1108
	53.142	1.7229	1.7234
	56.664	1.6239	1.6248
	62.21	1.4918	1.4925
$Zn_{0.75}Cu_{0.25}Fe_2O_4$	29.9547	2.9821	2.9851
	35.3146	2.5408	2.5457
	36.9433	2.4324	2.4347
	42.8465	2.1100	2.1108
	53.21	1.7209	1.7234
	56.6971	1.6230	1.6248
	62.2277	1.4914	1.4925
$Zn_{0.5}Cu_{0.5}Fe_2O_4$	30.3572	2.9435	2.9851
	35.6702	2.5163	2.5457
	37.393	2.4042	2.4347
	43.3111	2.0884	2.1108
	53.7481	1.7049	1.7234
	57.102	1.6125	1.6248
	62.6886	1.4813	1.4925
$Zn_{0.25}Cu_{0.75}Fe_2O_4$	30.1933	2.9591	2.9851
	35.5827	2.5223	2.5457
	37.2095	2.4156	2.4347
	43.1625	2.0952	2.1108
	53.5478	1.7108	1.7234
	57.0276	1.6144	1.6248
	62.6281	1.4828	1.4925

This is due to the decrease in the densities of nucleation centres in the doped samples which results in the formation of larger crystallite size[14]. The average crystallite size was determined with the use of the Scherrer's equation.

SEM Analysis*:* Figures-2(a),(b) and (c) show the SEM images for all the prepared samples of ferrites. The SEM show formation of the aggregated particles and also some vacant spaces within them. Porosity is located at the junctions of the aggregatess. It is evident that the grains of the Zn-Cu ferrite are very rough, and allow adsorption of oxygen on the surface. The results of the XRD and SEM pictures indicate all the samples are well crystalline-nano sized spinel ferrites.

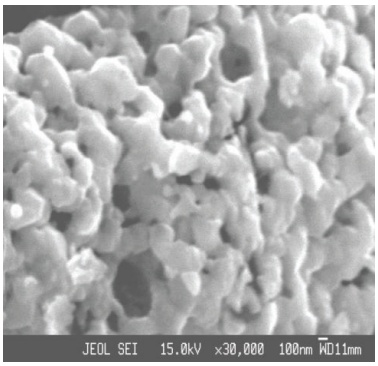

(a)

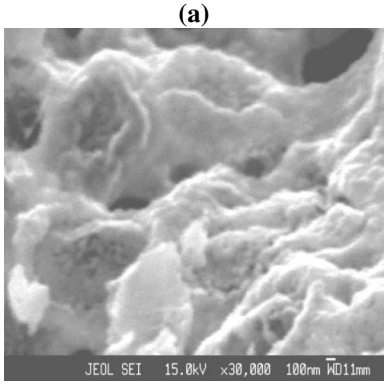

(b)

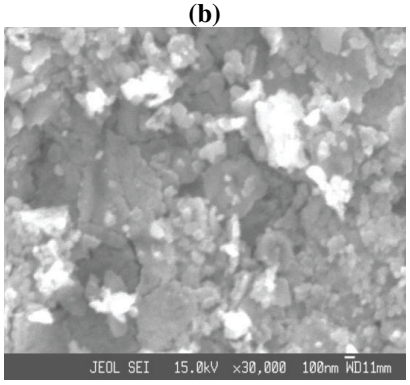

(c)

Figure-2
SEM micrographs of (a) $Zn_{1.0}Cu_{0\cdot0}Fe_2O_4$, (b) $Zn_{0.75}Cu_{0.25}Fe_2O_4$, and (c) $Zn_{0.25}Cu_{0.7}5Fe_2O_4$

FT-IR Analysis: FT-IR spectra of the synthesized ferrite nano particles measured in the frequency range of 400- 4,000 cm^{-1} are shown in Figure- 3. Two distinct bands at 410 and 630 cm^{-1}, are characteristic features of ferrospinels, and are attributed to the stretching vibration due to interactions between the oxygen atom and the cations in tetrahedral and octahedral sites, respectively. The difference between the two's is due to the changes in bond length (Fe-O) at the octahedral and tetrahedral sites. A sharp absorption band at around 630 cm^{-1} is due to the intrinsic vibrations of the tetrahedral groups and the other band the octahedral groups. There are two weak and broad absorptions around 1450 and 1680 cm^{-1} corresponding to the presence of small amount of residual carbon in the samples indicating that the residual carbon has mostly burnt away during the self-combustion process. The band positions of these absorptions indicate that this carbon is in the form of complex carbonates. Three distinct peaks are obtained at 1618 cm^{-1} (-C=O), 1316 cm^{-1} (C-O) and 795 cm^{-1} (La-O) suggest the presence of the oxalate ion. The IR spectra of the products after TG at 490^oC suggests incomplete decomposition as evident from peaks obtained at 1432, 1100, 1000 and 858cm^{-1}. A small peak at 1100cm^{-1} concurrent with diminution of oxalate peak suggest a carbonate like decomposition intermediate. A prominent peak at 1432cm^{-1} is due to the carbonate ion[13].

Thermal analysis: Thermogravimetric curves for lanthanum oxalate and its mixture with samples S1, S2, S3 and S4 shows significant increase in fractional decomposition α with respect to pure lanthanum oxalate although the decomposition temperature remain undisturbed i.e at 653K (figure-4). Mixture of lanthanum oxalate with S1 has low value of fractional decomposition α at the start of the decomposition compared with that of lanthanum oxalate but after attaining the temperature 683K the α value increases significantly till the completion of the reaction (Figure-4). However the incorporation of Cu in the Zn lattice the mixture of lanthanum oxalate with S2,S3 and S4 make the decomposition process facile with less value for decomposition temperture i.e 648K.It is found that $Zn_{0.75}Cu_{0.25}Fe_2O_4$ is the ideal composition showing highest value for α although the decomposition curves are indistinguishable in the graph. Under high resolution (figure-5) the trend follows the order S2>S4>S3.The Derivative curves are also shown in figure-signifying the temperature corresponding to the highest rate of decomposition α_{max} to be 659K.

Samples prepared with three different mole percentages of spinel ferrites S2 show trends with no remarkable change in fractional decomposition α. But at low concentration of catalyst (2 mol%), has highest α values than the others but as the temperature gradually increases upto 663K, 5 mol% and 10 mol% show equal activities but after that 10 mol% gets the higher value of fractional decomposition α till the completion of reaction (figure-6).

Kinetic analysis: The catalytic activity of mixed metal spinel ferrites of the Cu– Zn at the same temperatures was found to be

greater than that of Zn ferrite. The completion of reaction takes place in one step in case of pure lanthanum oxalate and so also its mixture with mixed metal spinel ferrites of the Cu– Zn,. For comparative study all the data are analysed for the one step process.

The kinetic parameters for the decomposition stage were determined using Coat-Redfern equation[15].

$$\log g(\alpha)/T^2 = \log(AR/\beta E) - E/2.0303RT \quad (1)$$

Where A is the pre exponential factor, β the heating rate, E the activation energy, R the universal gas constant and T the absolute temperature. $\log g(\alpha)/T^2$ is calculated for each possible rate controlling mechanisms using various solid state models and plotted against 1/T (figure-7 and 8), using best fit model for the reaction. The value of g(α) with highest coefficient of linear regression analysis, r gives the idea about the best fit mechanism. The best fit model F_3 i.e. the third order law is chosen for the entire temperature range 643-723K in order to compare all the data.

The activation energy, E and pre-exponential factor A were calculated from the slope and intercept respectively of the Coat-Redfern equation and the plausible mechanism and the corresponding kinetic and thermodynamic parameters are presented in table-2(a) and (b) using equations.

$$\Delta H^* = E - RT \quad (2)$$

$$\Delta S^* = R[\ln(hA/k_BT) - 1] \quad (3)$$

$$\Delta G^* = \Delta H^* - T\Delta S^* \quad (4)$$

ΔH^*, ΔS^* and ΔG^* are the enthalpy, entropy and free energy change of activation respectively.h is the plank's constant and k_B is the Boltzman's constant.

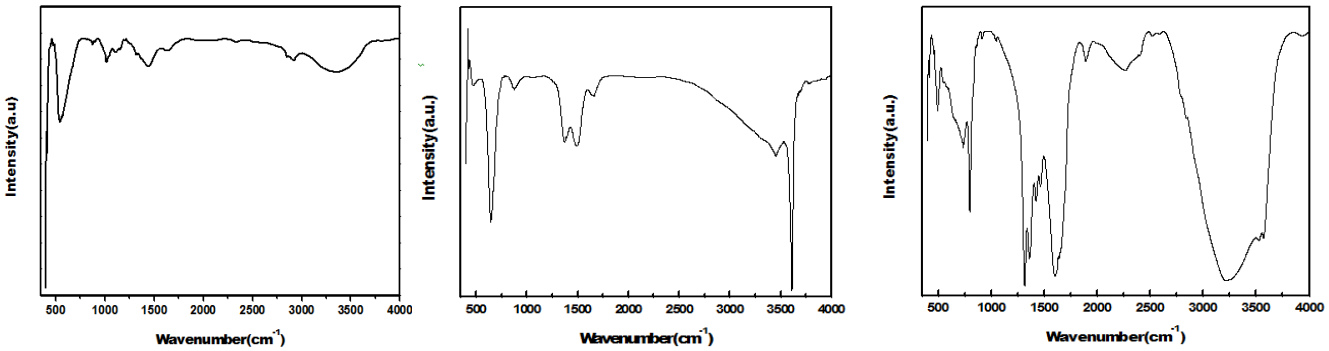

(a) **(b)** **(c)**

Figure-3

FTIR spectra of (a) $Zn_{0.75}Cu_{0.25}Fe_2O_4$ (b) $La_2(C_2O_4)_3$+ $Zn_{0.75}Cu_{0.25}Fe_2O_4$(Product after TG) (c) $La_2(C_2O_4)_3$+ $Zn_{0.75}Cu_{0.25}Fe_2O_4$(5 mol%)

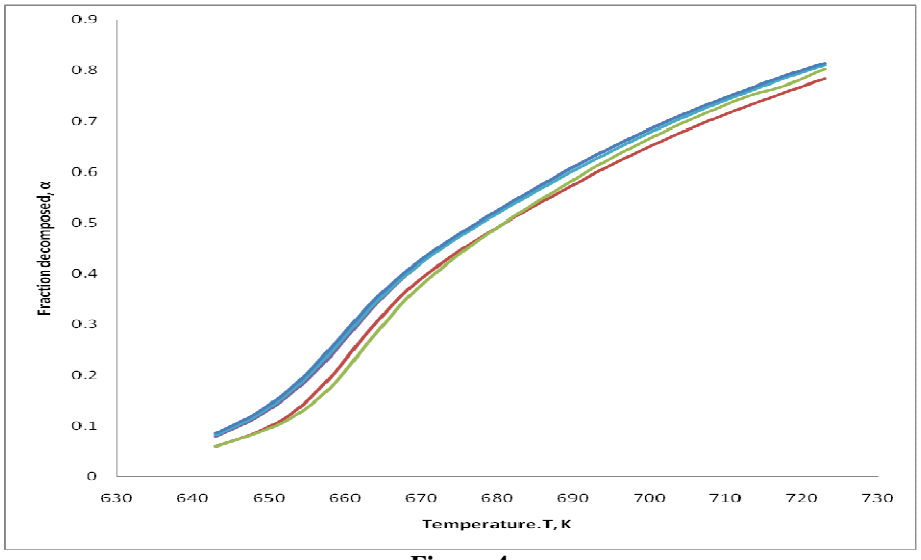

Figure-4

α-T curves for decomposition of Pure lanthanum oxalate(Red), lanthanum oxalate mixed with $ZnFe_2O_4$(5 mol%)-(Green), $Zn_{0.75}Cu_{0.25}Fe_2O_4$(5 mol%)- (Blue) $Zn_{0.5}Cu_{0.5}Fe_2O_4$(2 mol%)- (violet), $Zn_{0.25}Cu_{0.75}Fe_2O_4$(10 mol%)-Blue

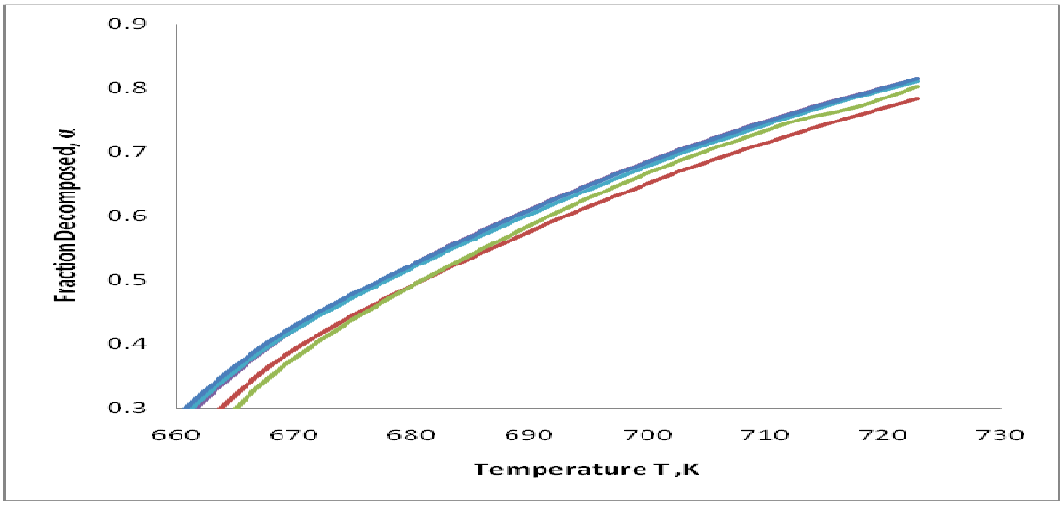

Figure-5
Enlarged α-T curves of Figure-4

Table-2(a)
Arrhenius parameters for the decomposition of various samples using Coat-Redfern equation

Samples	E(±0.05),Kjmol^{-1}	logA(±0.02),s^{-1}	k*(±0.05),s^{-1}	ΔH* KJmol^{-1}K^{-1}	ΔS* jmol^{-1}	ΔG* Kjmol^{-1}
$La_2(C_2O_4)_3$ Pure	135.523	10.26	0.3307	-130.044	-63.41	-87.242
$La_2(C_2O_4)_3$ +F1	146.609	11.16	0.3474	-141.131	-46.18	-109.959
$La_2(C_2O_4)_3$ +F2	147.681	11.29	0.3854	-142.202	-43.69	-112.711
$La_2(C_2O_4)_3$ +F3	144.024	10.96	0.3512	-138.545	-50.61	-104.383
$La_2(C_2O_4)_3$ +F4	145.384	11.11	0.3872	-139.905	-47.14	-108.085

Table-2(b)
Arrhenius parameters for the decomposition of various samples using Coat-Redfern equation

Samples	E(±0.05),Kjmol^{-1}	logA(±0.02),s^{-1}	k*(±0.05),s^{-1}	ΔH* Jmol^{-1}K^{-1}	ΔS* jmol^{-1}	ΔG* Kjmol^{-1}
$La_2(C_2O_4)_3$+F4(2mol%)	163.650	12.65	0.479	-158.171	-17.56	-146.318
$La_2(C_2O_4)_3$+F4(5mol%)	145.384	11.11	0.3872	-139.905	-47.14	-108.085
$La_2(C_2O_4)_3$+F4(10mol%)	161.678	12.45	0.4331	-156.199	-21.48	-141.700

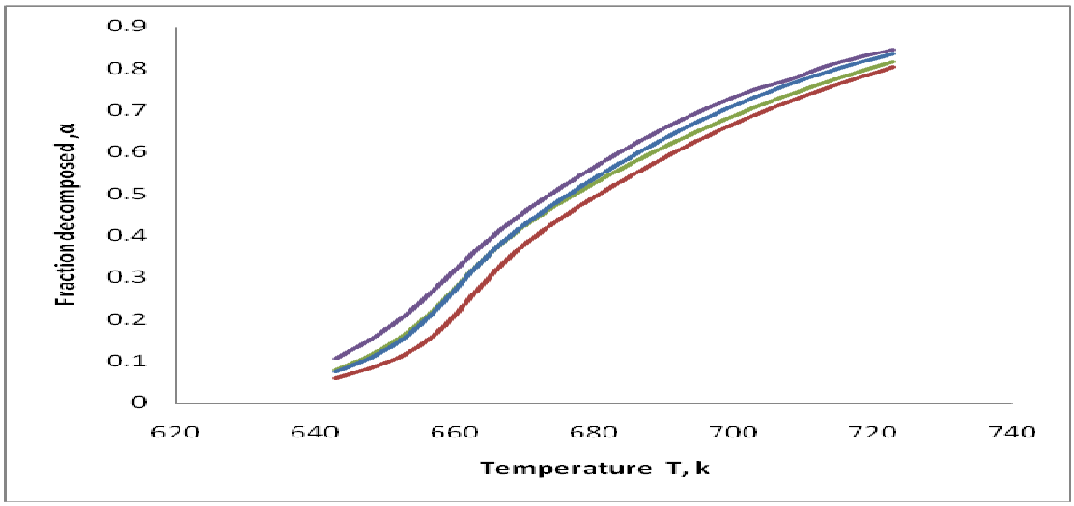

Figure-6
α-T curves for decomposition of lanthanum oxalate mixed with $ZnFe_2O_4$(5 mol%)-(red), $Zn_{0.75}Cu_{0.25}Fe_2O_4$(5 mol%)-(Green) $Zn_{0.75}Cu_{0.25}Fe_2O_4$(2 mol%)- (violet), $Zn_{0.75}Cu_{0.25}Fe_2O_4$(10 mol%)-Blue

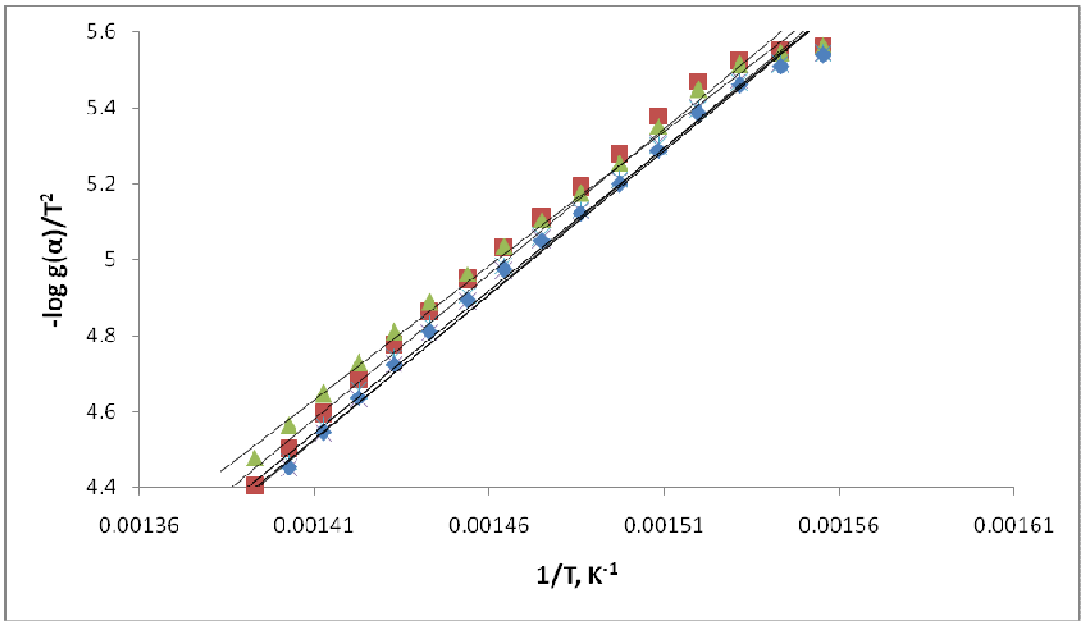

Figure-7
Variation of -log g(α)/T^2 against 1/T using F3 mechanism for the various samples $La_2(C_2O_4)_3$+$ZnFe_2O_4$(5 mol%)-Red, $La_2(C_2O_4)_3$-Green, $La_2(C_2O_4)_3$+$Zn_{0.75}Cu_{0.25}Fe_2O_4$(5 mol%)-Blue $La_2(C_2O_4)_3$+$Zn_{0.5}Cu_{0.5}Fe_2O_4$(5 mol%)-Star $La_2(C_2O_4)_3$+$Zn_{0.25}Cu_{0.75}Fe_2O_4$(5 mol%)-Star

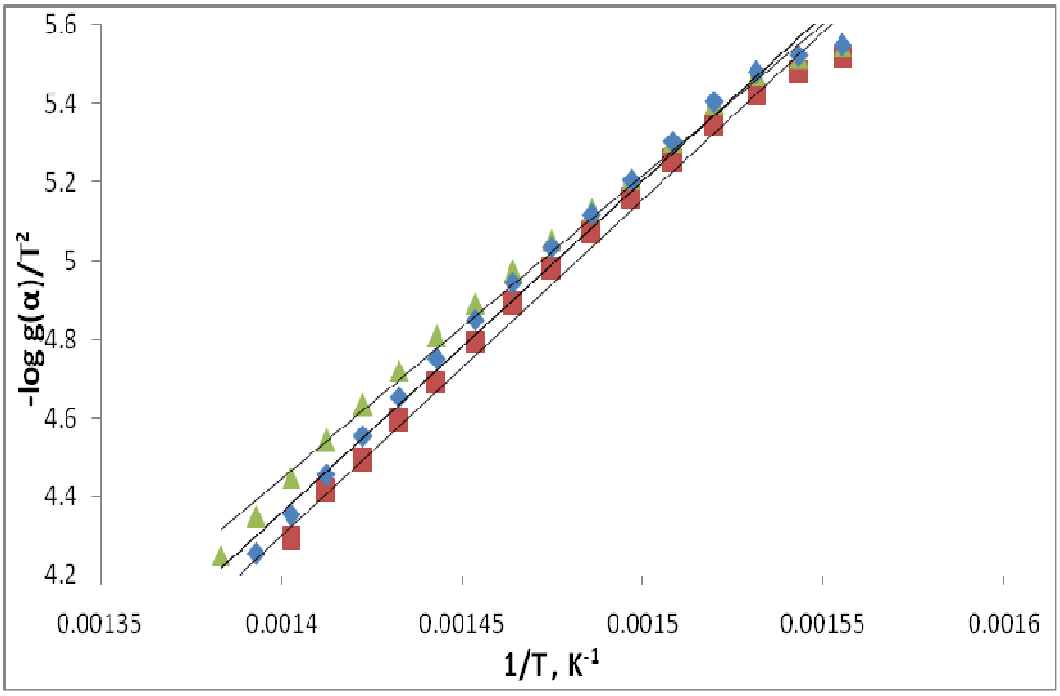

Figure-8
Variation of -log g(α)/T^2 against 1/T using F3 mechanism for the various samples $Zn_{0.75}Cu_{0.25}Fe_2O_4$(2 mol%)-Red, $Zn_{0.75}Cu_{0.25}Fe_2O_4$(5 mol%)-Green, $Zn_{0.75}Cu_{0.25}Fe_2O_4$(10 mol%)-Blue

The rate of the reaction was determined corresponding to the highest value of fraction decomposed i.e α_{max} and the corresponding temperature Ts in the DTG plots (figure-9) whose value is 675K.The rate constant k has got the highest value for S4 almost same as that of S2 with 5 mol% concentration and highest value may be attributed to high copper concentration.

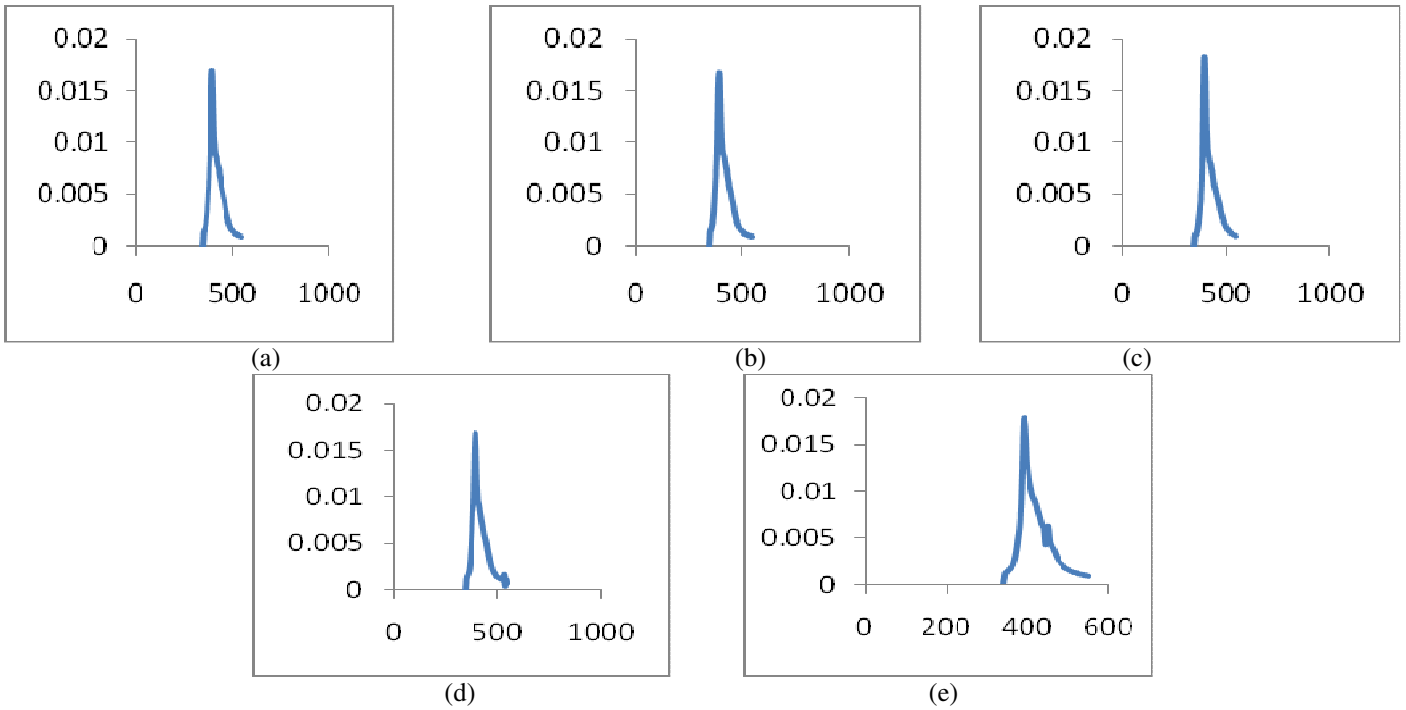

Figure-9
DTG plots(T vs dα/dt) of different samples Lanthanum Oxalate(a),Lanthanum Oxalate+$ZnFe_2O_4$(b), Lanthanum Oxalate+$Cu_{0.25}Zn_{0.75}Fe_2O_4$(c), Lanthanum Oxalate+ $Cu_{0.5}Zn_{0.5}Fe_2O_4$(d), Lanthanum Oxalate +$Cu_{0.75}Zn_{0.25}Fe_2O_4$(f)

The higher catalytic activity is attributed to, creation of new ion pairs Cu^{2+} –Fe^{+} and Cu^{+} –Fe^{2+} which increase the activities of the mixed ferrites and these forms are also called the mixed sites .These are present along with one component sites Cu^{2+} –Cu^{+}, Fe^{3+} –Fe^{2+} .The ion pairs are formed due to mutual charge interaction.

$C_2O_4^{2-} \rightarrow C_2O_4^{-} + e$ (1)
$Cu^{2+} + e \rightarrow Cu^{+}$ (2)
$Fe^{3+} + e \rightarrow Fe^{2+}$ (3)
$Cu^{+} + Fe^{3+} \rightarrow Cu^{2+} + Fe^{2+}$ (4)

Role played by the spinel ferrites: In $Zn_xFe_{3-x}O_4$,the ferrite can be presented with the formula $(Zn_x^{2+}Fe^{3+}_{1-x})_{tetra}$ $[Fe^{3+}_{1+x}Fe^{2+}_{1+x}]_{octa}O_4$, as the spinel structure is preserved in the range $0 \le x \le 1$[16]. Samples having higher zinc concentration there is weak tetrahedral A-site and octahedral B-site super exchange interaction. The conduction at lower temperature is due to hopping of electrons between Fe^{3+} and Fe^{2+} ions, whereas at higher temperature due to polaron hopping[17]. In addition, the increase of Zn content is associated with a decrease in copper content. In turn the possibility of Cu^{+} formation and $Cu^{2+} \leftrightarrow Cu^{1+}$ hopping process and the number of holes involved will be reduced. While heating $CuFe_2O_4$ sample, the concentration of B-site Cu^{2+} ions is increased at higher temperature. This reaction gives n-type conduction because of interstitial cation exchange given as

$Cu_A^{2+} + Fe_B^{3+} \rightarrow Cu_B^{2+} + Fe_A^{3+}$ (5)

The conduction mechanism for $CuFe_2O_4$ at lower temperature is p-type depending on the relative concentration of Cu^{1+} of Cu^{2+} ions on A-site. Zinc content is increased, tend to decrease Cu content at A-site .

$Cu_A^{1+} + Cu_A^{2+} \rightarrow Cu_A^{2+} + Cu_A^{1+}$ (6)

The $Cu_{1-x}Zn_xFe_2O_4$ system has a cubic spinel configuration with unit cell consisting of eight formula units of the form (Zn_xFe_{1-x}) A $[Cu_{1-x}Fe_{1+x}]$ B O_4. The Cu^{2+} ions have a preference for the octahedral sites and Zn^{2+} ions have preference for the tetrahedral sites[17]. The increasing of particle size with Zn content can be attributed to the large ionic radius of Zn^{2+} (0.84 Å) as compared to the ionic radius of Cu^{2+} (0.79Å). Hence Zn^{2+} replaces the smaller Cu^{2+} and change of catalytic activity of ferrite powders is obtained because of changes of the valence state of catalytically active components of the ferrite. The oxidation of carbon monoxide released from lanthanum oxalate, by metal ferrite as catalyst can be written in the following equations;

$La_2(C_2O_4)_3 \rightarrow La_2(CO_3)_3 + 3CO \rightarrow La_2O(CO_3)_2 + CO_2$ (7)
$La_2O(CO_3)_2 \rightarrow La_2O(CO_3) + CO_2$ (8)
$MFe_2O_4 + xCO \rightarrow MFe_2O_{4-x} + xCO_2$ (9)
$MFe_2O_{4-x} + 0.5xO_2 \rightarrow MFe_2O_4$ (10)

CO and O_2 diffuse to the surface of the ferrite and preferentially adsorb on its surface. This is a chemisorptions process of gas molecules and the oxygen in the ferrite transfer from the bulk to the chemisorbed species. CO_2 is produced by the reaction of CO and O_2 on the surface of the catalyst and then released from the

interface and leave sites for other CO and O_2 gas molecules adsorption.

Conclusions

i. The mixed ferrite of copper and zinc behaves as n-type semiconductor. ii. There is a decrease in transition of structure from tetragonal to cubic as the Zn content in the ferrite increases. iii. The conduction at lower temperature is due to hopping of electrons between Fe^{3+} and Fe^{2+} ions, whereas at higher temperature due to polaron hopping. iv. Formation of single phase spinel structure is confirmed at very low annealing temperature from XRD data, where there is no secondary phases. The particle size decreases with increasing Zn concentration probably due to the reaction temperature and time. v. The lattice size increase with increasing Zn content, which is due to large ionic radii of zinc in comparison to copper ions. vi. The increase in Zinc content increases particle size thereby providing comparatively. Less surface area for the catalytic activities, hence $Zn_{0.25}Cu_{0.75}Fe_2O_4$ is the best suitable catalyst out of the fours.

References

1. Sugimoto M, The past, present and future of ferrites, *Journal of the American Ceramic Society,* **82,** 269-280. **(1999)**

2. Suzuki Y., Epitaxial Spinel ferrite thin Films, *Annual Review of Material Research,* **31,** 265-289, **(2001)**

3. H. Nayak and Ashish K. Jena, Catalyst Effect of Transition Metal Nano Oxides on the Decomposition of Lanthanum Oxalate Hydrate: A Thermo gravimetric Study, *International Journal of Science and Research (IJSR) ,* **3(11),** 381-388 **(2014)**

4. Rakesh Kumar Singh, A. Yadav, Kamal Prasad and A. Narayan, Dependence of magnetic and structural properties of $Ni_{0.5}$ $M_{0.5}$ Fe_2O_4 (M=Co, Cu) nanoparticles synthesized by citrate precursor method on annealing temperature, *International Journal of Engineering, Science and Technology,* **2(8),** 73-79 **(2010)**

5. Joelda Dantasa, Jakeline Raiane D. Santosa, Rodrigo Bruno L. Cunhaa, Ruth Herta G. A. Kiminamib and Ana Cristina F. M. Costaa, Use of Ni-Zn ferrites doped with Cu as catalyst in the transesterification of soybean oil to methyl esters, *Materials Research,* **16(3),** 625-627 **(2013)**

6. Prabhulkar S.G. and Patil R.M Synthesis, Characterization and Catalytic Properties of Nickel Substituted Copper Ferrospinel nanoparticles, *Research Journal of Material Sciences,* **1(4),** 18-21, **(2013)**

7. H. Nayak, Kinetic and Thermodynamic Studies on the Non-Isothermal Decomposition of Lanthanum Oxalate Hydrate, Catalysed By Transition Metal Nano Oxides, *IOSR Journal of Applied Chemistry (IOSR-JAC),* **7(11),** 15-23 **(2014)**

8. Ch. Vinuthna, D. Ravinder, R. Madhusudan Raju D. Ravinder, Characterization of $Co_{1-X}Zn_xFe_2O_4$ Nano Spinal Ferrites Prepared By Citrate Precursor Method, *Int. Journal of Engineering Research and Applications,* **3(6),** 654-660 **(2013)**

9. Gopathi Ravi Kumar, Katrapally Vijaya Kumar, Yarram Chetty Venudhar, Synthesis, Structural and Magnetic Properties of Copper Substituted Nickel Ferrites by Sol-Gel Method, *Materials Sciences and Applications*, **3,** 87-91 **(2012)**

10. C.O. Ramankutty and S. Sugunan, Surface properties and catalytic activity of ferrospinels of nickel, cobalt and copper, prepared by soft chemical methods, *Applied Catalysis A: General,* **218**, 39-51 **(2001)**

11. Anjaneyulu T., Narayana Murthy P., Narendra K and Vijaya Kumar, Structural and Magnetic Properties of $Cu_{1-X}Zn_XFe_2O_4$Nano-powders synthesised by Oxalate based precursors method *International Journal of Basic and Applied Chemical Sciences*, **3(1),** 50-59 **(2013)**

12. Hussain Abd-Elkariem Dawoud, Thermoelectric Power of Cu-Zn Ferrites, *Materials Sciences and Applications,* **2,** 1572-1577 **(2011)**

13. Nayakv H., Pati S.K. and Bhatta D., Decomposition of γ-irradiated $La_2(C_2O_4)_3 + CuO$ mixture: a non-isothermal study. *Radiation effects and defects in solids,* **159,** 93-106 **(2004)**

14. Anuj Jain, Ravi Kant Baranwal, Ajaya Bharti, Z. Vakil, and C.S. Prajapati., Study of Zn-Cu Ferrite Nanoparticles for LPG Sensing, *The ScientificWorld Journal, Volume 2013, Article ID 790359*

15. Nayak H. and Bhatta D., Catalytic effects of magnesium chromite spinel on the decomposition of lanthanum oxalate,*Thermochim Acta,* **389(1-2),** 109-119 **(2002)**

16. Koleva K.V., Velinov N.I., Tsoncheva T.S., Mitov I.G. and Kunev B.N., Preparation, structure and catalytic properties of $ZnFe_2O_4$, *Bulgarian Chemical Communications,* **45(4),** 434–439 **(2013)**

17. Hussain Abd-Elkariem Dawoud, Thermoelectric Power of Cu-Zn Ferrites, *Materials Sciences and Applications*, **2,** 1572-1577 **(2011)**